Dispersion Analysis of Smoothed Particle Hydrodynamics to Study Convergence and Numerical Phenomena at Coarse Resolution

Olga Stoyanovskaya[1], Vadim Lisitsa[2(✉)], Sergey Anoshin[3], and Tamara Markelova[1]

[1] Boreskov Institute of Catalysis SB RAS, Lavrentiev Ave. 5, Novosibirsk 630090, Russia
[2] Institute of Mathematics SB RAS, Koptug Ave. 4, Novosibirsk 630090, Russia
lisitsavv@ipgg.sbras.ru
[3] Novosibirsk State University, Pirogova, 2, Novosibirsk 630090, Russia
s.anoshin@g.nsu.ru

Abstract. The Smoothed Particle Hydrodynamics (SPH) method is a meshless Lagrangian method widely used in continuum mechanics simulation. Despite its wide application, theoretical issues of SPH approximation, stability, and convergence are among the unsolved problems of computational mathematics. In this paper, we present the application of dispersion analysis to the SPH approximation of one-dimensional gas dynamics equations to study numerical phenomena that appeared in practice. We confirmed that SPH converges only if the number of particles per wavelength increases while smoothing length decreases. At the same time, reduction of the smoothing length when keeping the number of particles in the kernel fixed (typical convergence results for finite differences and finite elements) does not guarantee the convergence of the numerical solution to the analytical one. We indicate the particular regimes with pronounced irreducible numerical dispersion. For coarse resolution, our theoretical findings are confirmed in simulations.

Keywords: Smoothed particles hydrodynamics (SPH) · Numerical dispersion · Convergence analysis

1 Introduction

The SPH method is a meshless Lagrangian method for solving continuum mechanics problems or systems of partial differential equations written in the

V.L. did the dispersion analysis under the support of Russian Science Foundation grant no. 21-71-20003, O.S. performed numerical experiments, and T.M. did the asymptotic analysis; O.S. and T.M. work were founded by Russian Science Foundation grant no 21-19-00429, S.A. visualized the results.

© The Author(s), under exclusive license to Springer Nature Switzerland AG 2022
O. Gervasi et al. (Eds.): ICCSA 2022, LNCS 13375, pp. 184–197, 2022.
https://doi.org/10.1007/978-3-031-10522-7_14

divergence-free form. The SPH method was suggested in [7,12] and is used in astrophysics, ballistics, volcanology, oceanography, and many other applications nowadays [15]. It synergetically couples with other numerical techniques, e.g., particle-in-cell approaches for solving stiff problems [23,24]. Several multiphysics commercial [28] and freeware codes [8,9,19,22,26] have been developed on its basis. In the SPH method, a continuous medium is replaced by a discrete set of particles. These particles are moving interpolation nodes for spatial derivatives computation. The spatial derivatives of a function given at moving nodes irregularly located nodes are calculated using a smooth non-linear function (kernel). The kernel is nonzero in a bounded region called the kernel support domain. The accuracy of the spatial derivative computation is determined by two numerical parameters - the average distance between the interpolation nodes and the average size of the support domain or the smoothing length. Due to the irregular distribution of model particles in space and the non-linearity of the kernel, it is challenging to study the properties of the SPH method theoretically. Therefore, the theoretical issues of approximation, stability, and convergence are among the unsolved problems of the SPH method [25].

Dispersion analysis is a powerful tool that allows directly estimating the convergence of the numerical solution to a plane wave solution admitted by the original system of hyperbolic differential equations [5]. This approach is widely used in seismic modeling to choose appropriate grid steps or to construct dispersion suppressing schemes which can be used with extremely coarse discretizations (close to 2.5 points per wavelength) [11]. If applied to finite elements [17], discontinuous Galerkin [2,10], or spectral elements [13] dispersion allows estimating the convergence rate of the numerical solution, studying the artificial modes, and also performing the stability analysis. Analysis of the numerical dispersion caused by SPH approximation was also reported in [4,6,14–16,20] Dispersion analysis of SPH is based on the assumption of a liner small-amplitude wave propagation. Thus, the particles are supposed to oscillate near a fixed position, and the problem can be linearized, and relative phase velocity error can be estimated depending on the distance between the particles and the kernel size.

This paper presents the dispersion analysis of the SPH approximation of one-dimensional gas dynamics equations. First, we consider the basic classical form of the SPH (1) with a constant smoothing length, (2) with guaranteed mass and momentum conservation in the whole computational domain, (3) without artificial viscosity. Then, we provide the formula for the numerical velocity of propagation of a sound wave, which is a function of three independent variables: wavelength, the distance between the unperturbed particles, and the kernel length. Finally, we prove that the phase velocity of the SPH plane-wave solution converges to that of the solution of the differential equations; both kernel length and the inter-particle distance tend to zero simultaneously, which confirms the results of [6,20,21,27]. However, if the distance between the particles tends to zero with a fixed kernel length, the dispersion error may not converge to zero, resulting in irreducible phase error.

The paper has the following structure. We formulate the problem in Sect. 2. Construction of the phase velocity of the numerical solution is presented in Sect. 3. Numerical experiments are provided in Sect. 4.

2 Statement of the Problem

2.1 System of Gas Dynamics

Consider system of equations describing dynamics of viscous compressible gas

$$\begin{aligned} &\frac{\partial \rho_{\mathrm{g}}}{\partial t} + \vec{v} \cdot \nabla \rho_g = -\rho_{\mathrm{g}} \nabla \cdot \vec{v}, \\ &\frac{\partial v}{\partial t} + \vec{v} \cdot \nabla \vec{v} = -\frac{1}{\rho_{\mathrm{g}}} \nabla p, \\ &p = c_{\mathrm{s}}^2 \rho_{\mathrm{g}}, \end{aligned} \tag{1}$$

where ρ_g is the gas mass density, $\vec{v}$ is the gas velocity, p is pressure, c_s is the speed of sound.

We consider a small perturbation of the solution in the vicinity of the stationary mode; that is $\rho_g = \rho^0 + \delta\rho$ and $\vec{v} = \delta\vec{v}$. Thus the system can be linearized as

$$\frac{\partial \delta\rho_{\mathrm{g}}}{\partial t} + \rho_{\mathrm{g}}^0 \nabla \cdot \delta\vec{v} = 0, \; \rho_{\mathrm{g}}^0 \frac{\partial \delta\vec{v}}{\partial t} + c_s^2 \nabla \delta\rho_{\mathrm{g}} = 0, \tag{2}$$

where $\delta\rho_g$ is the density perturbation, $\delta\vec{v}$ is the velocity perturbation. In our further considerations we will deal with 1D statements; thus, system (2) can be rewritten as

$$\frac{\partial \delta\rho_{\mathrm{g}}}{\partial t} + \rho_{\mathrm{g}}^0 \frac{\partial \delta v}{\partial x} = 0, \; \rho_{\mathrm{g}}^0 \frac{\partial \delta\vec{v}}{\partial t} + c_s^2 \frac{\partial \delta\rho_{\mathrm{g}}}{\partial x} = 0. \tag{3}$$

System (3) admits a plane-wave solution of the form

$$\begin{pmatrix} \delta\rho \\ \delta v \end{pmatrix} = \begin{pmatrix} \tilde{\rho} \\ \tilde{v} \end{pmatrix} e^{i(kx - \omega t)}.$$

if time-frequency ω and wavenumber k satisfy the dispersion relation

$$\omega^2 - c_s^2 k^2 = 0.$$

In these notations $(\tilde{\rho}, \tilde{v})^T$ is the polarization vector which is nonzero. Using the definition of the phase velocity, one gets

$$c \equiv \frac{\omega}{\|k\|} = \pm c_s.$$

and corresponding polarization vectors are:

$$\begin{pmatrix} \tilde{\rho} \\ \tilde{v} \end{pmatrix} = \begin{pmatrix} \rho_{\mathrm{g}}^0 \\ \pm c_s \end{pmatrix}$$

In our study, we focus on the phase velocity and the error in the phase velocity induced by the SPH approximation of Eq. 1).

2.2 Smoothed Particle Hydrodynamics Method

Following [15,18] semi-discrete formulation of smooth particle hydrodynamics method applied to 1D case of system (1) can be written as

$$\begin{aligned} &\frac{dx_a}{dt} = v_a, \\ &\rho_a = M \sum_{b=a-B}^{a+B} W_{a,b}, \\ &\frac{dv_a}{dt} = -M \sum_{b=a-B}^{a+B} \left(\frac{P_a}{\rho_a^2} + \frac{P_b}{\rho_b^2} \right) \frac{\partial W_{a,b}}{\partial x_a}, \\ &P_a = c_s^2 \rho_a, \end{aligned} \tag{4}$$

where x_a is the particle coordinate, x_b are coordinates of the neighbour particles which are involved in the local stencil, ρ_a and v_a are mass density and velocity of the a-th particle, M is a particle mass (same for all particles), B is the half of the number of neighbours (for equally spaced particles). Function $W_{a,b} = W(x_a - x_b, H)$ is the kernel function, which defines the properties of particular SPH approximation. The kernel is even function with respect to x_a; which is $W_{a,b} = W(x_a - x_b, H) = W(x_b - x_a, H) = W_{b,a}$. It is finite function with limited support and it is smooth enough. Moreover, $W_{a,b}$ tends to Dirac delta function as $x_b - x_a$ tends to zero.

In this study we consider the kernel function based on the cubic splines interpolation:

$$W_{a,b} = \frac{2}{3\,H} \begin{cases} 1 - \frac{3}{2} \left(\frac{|x_a - x_b|}{H} \right)^2 + \frac{3}{4} \left(\frac{|x_a - x_b|}{H} \right)^3, & \frac{|x_a - x_b|}{H} \in [0, 1], \\ \frac{1}{4} \left(2 - \frac{|x_a - x_b|}{H} \right)^3, & \frac{|x_a - x_b|}{H} \in [1, 2], \\ 0, & \frac{|x_a - x_b|}{H} > 2. \end{cases} \tag{5}$$

3 Numerical Dispersion

Numerical dispersion measures the error caused by the numerical method in the phase velocity of a plane wave solution. On the other hand, it can be considered as a direct method to estimate the convergence of the numerical solution to the plane wave solution [1,3,5,10]. To estimate the numerical dispersion, one needs to construct the plane wave solution of the linearized system (4).

To construct a plane-wave solution of system (4) we follow the approach of [4]. Assume that we seek for the small perturbation of the solution of the form:

$$\begin{aligned} x_a &= a\Delta x + X e^{i(k x_a - \omega t)}, \\ \rho_a &= \rho_0 + R e^{i(k x_a - \omega t)}, \\ v_a &= V e^{i(k x_a - \omega t)}. \end{aligned} \tag{6}$$

where Δx is the unperturbed distance between the particles, X, R, and V are the unknown components of the polarization vector.

Substituting relations (6) into the system (4) and neglecting the high-order terms one gets the system of linear equations with respect to the polarization vector components:

$$i\omega X + V = 0,$$
$$R = MX \sum_{b=a-B}^{a+B} (1 - e^{ik(x_b - x_a)}) \frac{\partial W_{a,b}}{\partial x_a},$$
$$V = \frac{M}{i\omega} \frac{c_s^2}{\rho_0} \sum_{c=a-B}^{a+B} \left(-\frac{R}{\rho_0} (1 + e^{ik(x_c - x_a)}) \frac{\partial W_{a,c}}{\partial x_a} + 2X(1 - e^{ik(x_c - x_a)}) \frac{\partial^2 W_{a,c}}{\partial x_a^2} \right).$$

If one requires the system to posses nontrivial solution; thus, the determinant to be equal to zero one may construct the dispersion relation:

$$\omega^2 - 8M \frac{c_s^2}{\rho_0} \sum_{b=0}^{B} \sin^2(kr_b/2) \frac{\partial^2 W_{a,b}}{\partial r_b^2} + 4M^2 \frac{c_s^2}{\rho_0^2} \left[\sum_{b=0}^{B} \sin(kr_b) \frac{\partial W_{a,b}}{\partial r_b} \right]^2 = 0. \quad (7)$$

where $r_b = x_b - x_a = (b - a)\Delta x$. Using the definition of the phase velocity one gets:

$$c_s^{SPH} = \pm c_s \sqrt{\frac{8M}{k^2 \rho_0} \sum_{b=0}^{B} \sin^2(kr_b/2) \frac{\partial^2 W_{a,b}}{\partial r_b^2} - \frac{4M^2}{k^2 \rho_0^2} \left[\sum_{b=0}^{B} \sin(kr_b) \frac{\partial W_{a,b}}{\partial r_b} \right]^2} = 0. \quad (8)$$

3.1 Asymptotic Analysis

The first step in the dispersion analysis of the SPH should be consideration of the limiting case of $\Delta x \to 0$.

Consider

$$\lim_{\Delta x \to 0} (c_s^{SPH})^2 = -c_s^2 \left(\int_{-\infty}^{+\infty} \frac{\sin(kr)}{k} \frac{\partial W}{\partial r} dr \right)^2 + c_s^2 \int_{-\infty}^{+\infty} \frac{\sin^2(\frac{kr}{2})}{(\frac{k}{2})^2} \frac{\partial^2 W}{\partial r^2} dr \quad (9)$$
$$= c_s^2 \mathcal{F}[W] (2 - \mathcal{F}[W])$$

where $\mathcal{F}[W](k)$ is the Fourier transform of the kernel function. For the cubic spline kernel, provided by Eq. 5) the Fourier transform is known (see e.g. [18]) and the limit can be represented as:

$$\lim_{\Delta x \to 0} \frac{\omega_{SPH}^2}{k^2} = c_s^2 \frac{\sin^4(\frac{kH}{2})}{(\frac{kH}{2})^4} \left(2 - \frac{\sin^4(\frac{kH}{2})}{(\frac{kH}{2})^4} \right) \quad (10)$$

Thus, it is seen that when Δx tends to zero simultaneously with kH tends to zero, c_s^{SPH} tends to c_s, and convergence of the numerical solution to analytical one takes place. However, any fixed H SPH possesses irreducible error even if Δx tends to zero. Moreover, this error has a pronounced impact when $kH > 10$. Below we study the irreducible error in detail.

3.2 Dimensionless Variables

We consider the linear wave propagation process; thus, it is convenient to introduce the dimensionless variables, describing the discretization. Originally, defining SPH approximation, two variables were introduced. They are the distance between the particles Δx and the smoothing length H, considered as the stencil length in analogy with finite differences. However, the number of grid points per wavelength is typically used for the dispersion analysis. It is defined as $N = \dfrac{\lambda}{\Delta x} = \dfrac{2\pi}{k\Delta x}$, where λ is the wavelength. The other parameter which is convenient for the SPH method is the number of kernels per wavelength $K = \dfrac{2\pi}{kH}$. In addition, we introduce the parameter $\varphi = \dfrac{\Delta x}{H}$ representing the number of neighbors or points in a stencil. These three parameters are dependent, so we will deal with the pairs of (N, φ) or (K, φ) to characterize the discretization. It is clear that $K = \varphi N$.

Using these notations the phase velocity can be rewritten as

$$c_s^{SPH}(N,\varphi) = \frac{c_s N\varphi}{\pi}\sqrt{2\varphi\sum_{j=0}^{[2/\varphi]}\sin^2\left(j\frac{\pi}{N}\right)\tilde{W}_2(j\varphi) - \varphi^2\left[\sum_{j=0}^{[2/\varphi]}\sin\left(j\frac{2\pi}{N}\right)\tilde{W}_1(j\varphi)\right]^2}, \quad (11)$$

or

$$c_s^{SPH}(K,\varphi) = \frac{c_s K}{\pi}\sqrt{2\varphi\sum_{j=0}^{[2/\varphi]}\sin^2\left(j\varphi\frac{\pi}{K}\right)\tilde{W}_2(j\varphi) - \varphi^2\left[\sum_{j=0}^{[2/\varphi]}\sin\left(j\varphi\frac{2\pi}{K}\right)\tilde{W}_1(j\varphi)\right]^2}, \quad (12)$$

where

$$\tilde{W}_1(j\varphi) = H^2\frac{\partial W(r,H)}{\partial r}(j\Delta x, H) = \frac{2}{3}\begin{cases} -3j\varphi + \dfrac{9}{4}(j\varphi)^2, & j\varphi \in [0,1], \\ -\dfrac{3}{4}(2-j\varphi)^2, & j\varphi \in [1,2], \\ 0, & j\varphi > 2. \end{cases},$$

$$\tilde{W}_2(j\varphi) = H^3\frac{\partial^2 W(r,H)}{\partial r^2}(j\Delta x, H) = \frac{2}{3}\begin{cases} -3 + \dfrac{9}{2}j\varphi, & j\varphi \in [0,1], \\ \dfrac{3}{2}(2-j\varphi), & j\varphi \in [1,2], \\ 0, & j\varphi > 2. \end{cases}$$

Using formulae (11) and (12) one may estimate the phase velocities of the numerical solutions for working (coarse enough) discretizations, even if the asymptotic regime is not achieved.

4 Numerical Experiments

4.1 Numerical Analysis of the Dispersion Relations

First, we need to study the derived estimation of the phase velocities. We considered the linearized problem (3) with $c_s = 1$ and $\rho_g^0 = 1$. Thus, the exact phase velocity of the plane-wave solution of the differential equation equals one. Next, we computed phase velocity of the plane-wave solution of SPH problem (9), according to formulae (11) and (12). We assumed that parameter $\varphi = \Delta x/H \in [0, 1]$. The case of $\varphi \to 0$ corresponds to a fixed kernel length, but the distance between the particles tending to zero, which is $\Delta x \to 0$ for $H = const$. The case of $\varphi = 1$ corresponds to $\Delta x = H$, which means that the kernel includes only one neighboring point. This case is physically meaningless, but it allows illustrating the main problems of SPH approximation. Arbitrary fixed value of φ means that we fix the ratio $\Delta x/H$ or we fix the stencil to make the analysis close to that of finite differences or finite elements [1,10]. Parameters N and K representing the number of particles per wavelength and number of stencils per wavelength, respectively, may vary between 1 and ∞. The higher their values are, the fine the discretization is. In Fig. 1 we provide the plots of c_s^{SPH} as function of two variables, both (φ, N) and (φ, K). Note that phase velocity is a monotonous function of N or K, whereas its behavior as a function of φ is complex and requires detailed study. In addition, even for high values of N and K, phase velocity may strongly variate from one, i.e., from the correct value. Moreover, the velocity plot as a function of (φ, N) illustrates that for fixed N and low values of φ, velocity tends to zero, leading to 100% error. This case corresponds to the fixed distance between the particles Δx but reduces $\Delta x/H$. Thus, H increases and exceeds a wavelength, which causes the loss of any approximation. This effect is also observed in [21]. This effect can be seen in Fig. 2 where the phase velocity is provided as a function of φ for fixed $N = 100$ and $K = 100$. The plots illustrate the complex dependence of the phase velocity (relative error) on $\varphi = \Delta x/H$. It is not monotonous; moreover, it is not a smooth function. If a fixed N with $\varphi \to 0$ is considered, the error tends to be 100%, as discussed above.

The main effect that can be observed in Fig. 2 is the lack of convergence in the SPH method when φ is fixed. Indeed, the plots illustrate that for fine enough discretizations $K = 100$; which is 100 kernels per wavelength, and reasonable $\varphi \in [\varepsilon, 1]$ phase velocity error tends to be a constant different from zero. This leads to irreducible error in numerical solution; i.e., the plane wave propagates with an incorrect velocity which could not be corrected by mesh refinement with a fixed stencil or fixed number of neighbors. There are a set of local maximums where the error is close to zero; they are $\varphi = 1/P$, where P is an integer. The other local maximums $\varphi = 2/(2P + 1)$, where P is an integer. The error values in these points strongly deviate from zero, thus causing the irreducible error. To illustrate the influence of φ on error, we considered relative error as a

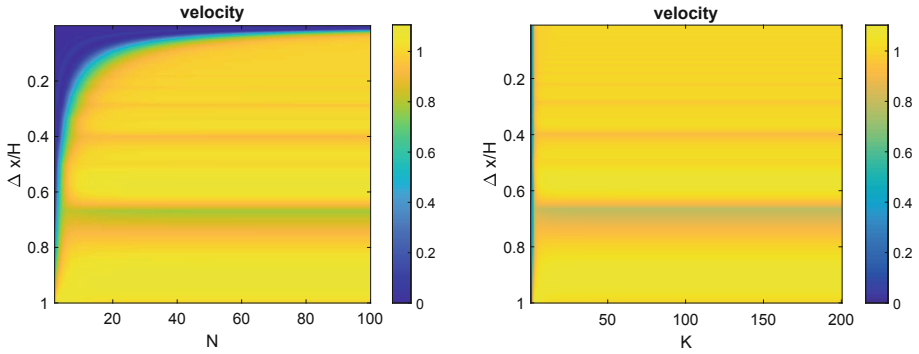

Fig. 1. Phase velocity of the SPH method as function of (φ, N) - left and (φ, K) - right.

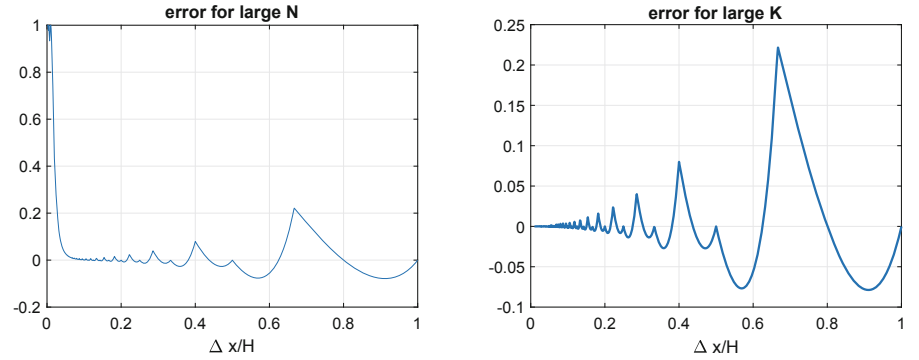

Fig. 2. Relative velocity error as function of $\varphi = \Delta x/H$ for fixed $N = 100$ - left, and $K = 100$ - right.

function of K for several fixed values of φ. In particular, we considered $\varphi = 0.5$ which corresponds to a local maximum, where the error tends to zero for large K; $\varphi = 2/3$ corresponding to local maximum deviating from zero; $\varphi = 0.569$ corresponding to one of the local minimums also deviating from zero, and $\varphi = 0.625$ corresponding to a point where the error is close to zero (not a local minimum). According to the presented results (Fig. 3), SPH converges with the second order, if $\varphi = 1/P$, where P is integer. However, for other values of φ, the error tends to some values, different from zero. These asymptotic are reached rather fast; i.e., for $K < 100$ and further mesh refinement does not improve the accuracy.

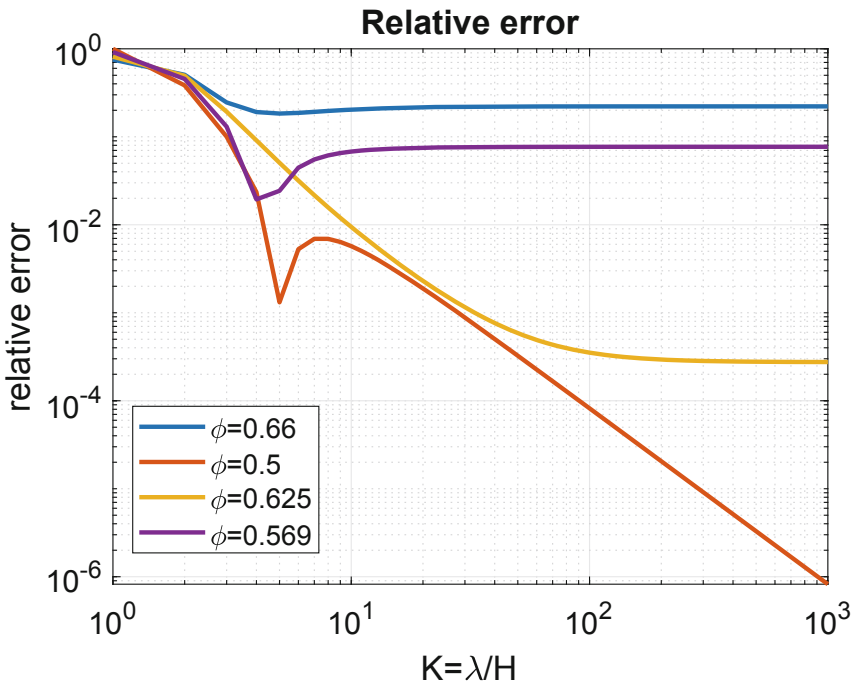

Fig. 3. Relative velocity error as function of K for fixed φ (in logarithmic scale).

The last but not least case which should be considered is fixed K with decreasing φ. It corresponds to the situation when the smoothing length H is fixed, but the distance between the particles Δx is refined. According to the plot in Fig. 2 convergence of the relative error is expected, however, in a non-monotonous way. To estimate the convergence rate, we considered relative error in local maximums $\varphi = 2/(2P + 1)$, where P is integer, as presented in Fig. 4. The results illustrate the second order of the maximum error reduction if $\varphi \to 0$. Additionally, we provide the plots of the relative error with respect to K for several values of φ corresponding to the local maximums (5). One may observe the reduction of the asymptotic error; moreover, the error converges to asymptotic with the second order with respect to K.

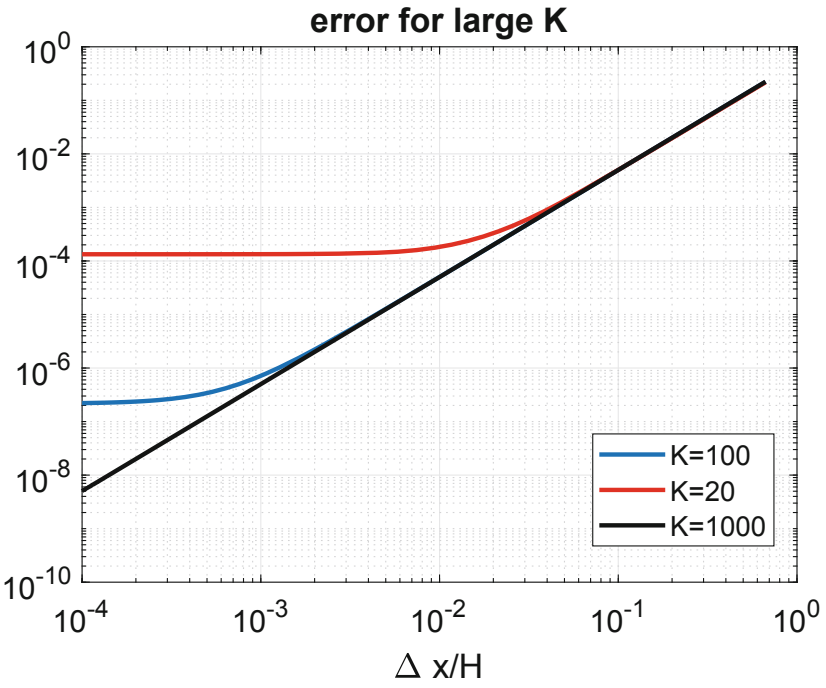

Fig. 4. Relative velocity error at local maximums $\varphi = 2/(2P+1)$, where P is integer for fixed K (in logarithmic scale).

4.2 Effect of Numerical Dispersion on Propagating Impulse

To illustrate the effect of the numerical dispersion of the solution, we simulated propagation of the Ricker wavelet

$$f(t) = (1 - 2\pi^2\nu_0^2 t^2)e^{-\pi^2\nu_0^2 t^2},$$

if the propagation velocity is constant and frequency-independent the solution propagates unperturbed along the characteristics; i.e., $u(t,x) = f(t - x/c_s)$. However, if the sound speed depends on the frequency, the pulse will be destructed, and the solution should be constructed as:

$$\tilde{f}(t - x/\hat{c}_g(\omega)) = \mathcal{F}^{-1}\left[e^{i\omega(t - x/\hat{c}_g(\omega))}\mathcal{F}[f(t)]\right],$$

where $\mathcal{F}$ is the Fourier transform with respect to time, and $c(\omega)$ is the phase velocity obtained from the dispersion analysis, $\hat{c}_g(\omega)$ is the frequency-dependent phase velocity. Ricker pulse is defined by its central frequency $\nu_0 = \frac{\omega_0}{2\pi}$, so that its spectra can be considered finite $\omega \in 2\pi[\nu_0/2, 2\nu_2]$. It means that if we fix the discretization with respect to the central frequency, the discretization will be coarser for high-frequency modes, and it will be finer for low-frequency models presented in the pulse.

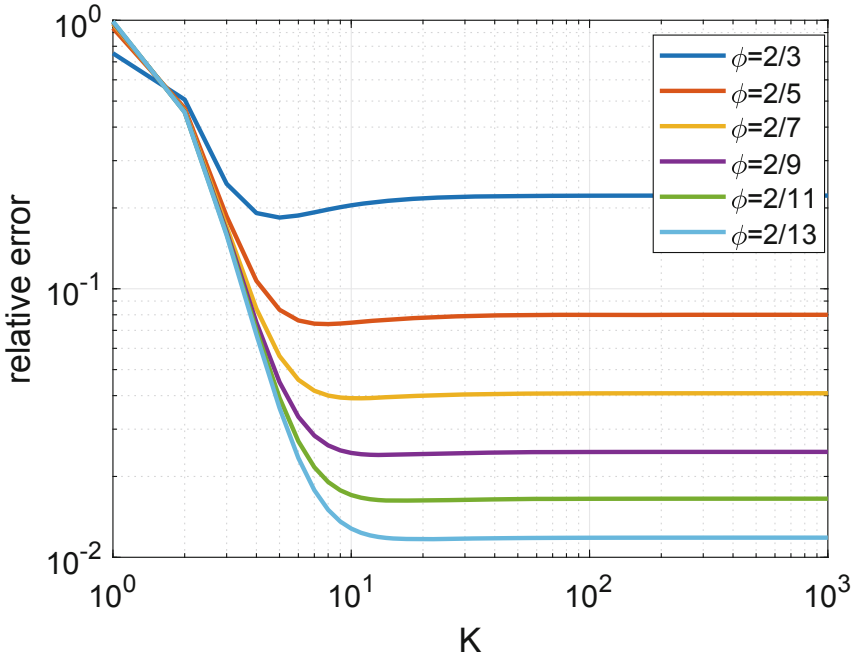

Fig. 5. Relative velocity error as function of K for fixed φ corresponding to local maximums (in logarithmic scale).

We considered the impulse propagated ten wavelengths (measured according to central frequency). We chose three discretizations $N = 50$ for all experiments, whereas φ varied. In particular Fig. 6 corresponds to $\varphi = 0.19$, Fig. 7 corresponds to $\varphi = 0.25$, and Fig. 8 corresponds to $\varphi = 0.2875$. In the first case, we observe significant dispersion in the signal because the phase velocity error tends to almost zero for $\varphi = 0.19$, but it still strongly depends on the discretization for $N \in [25, 100]$. Point $\varphi = 0.25$ corresponds to the local maximum of the error function, which equals zero. As a result, the numerical dispersion is small, and the impulse is almost not distorted. The last case of $\varphi = 0.2875$ corresponds to high irreducible phase velocity error. Moreover, the error is almost achieved its limit for the considered discretizations $N \in [25, 100]$. Thus, we observed almost no impulse distortion, but it propagated with incorrect velocity.

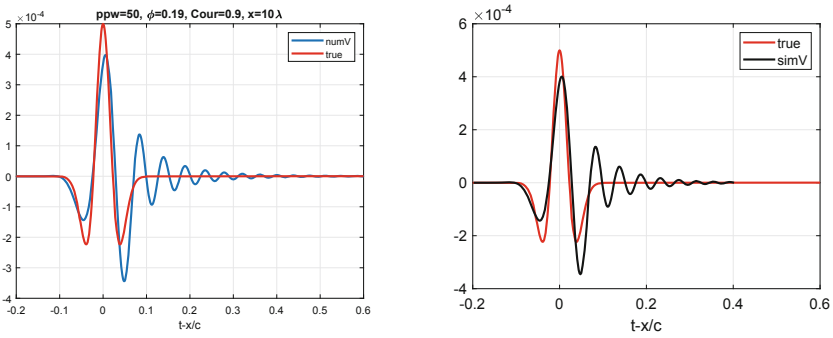

Fig. 6. Original impulse (red) and distortion of the impulse due to numerical dispersion. Left plot represents theoretical prediction, right plot represents numerical simulation results. Discretization was $N = 50$ and $\varphi = 0.19$. (Color figure online)

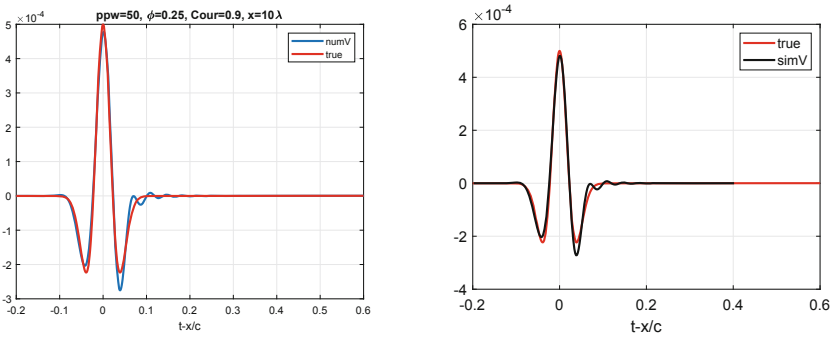

Fig. 7. Original impulse (red) and distortion of the impulse due to numerical dispersion. Left plot represents theoretical prediction, right plot represents numerical simulation results. Discretization was $N = 50$ and $\varphi = 0.25$. (Color figure online)

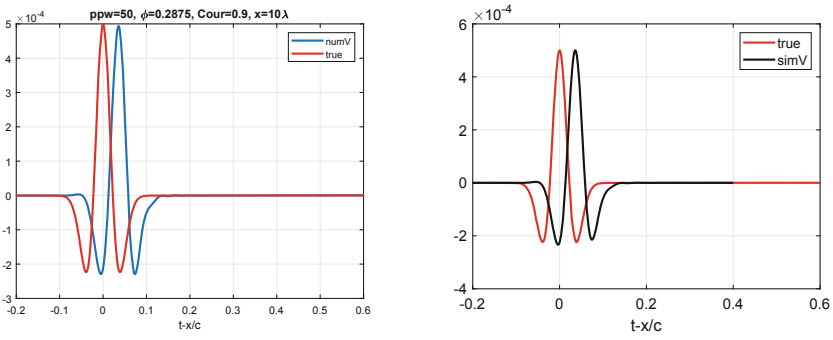

Fig. 8. Original impulse (red) and distortion of the impulse due to numerical dispersion. Left plot represents theoretical prediction, right plot represents numerical simulation results. Discretization was $N = 50$ and $\varphi = 0.2875$. (Color figure online)

5 Conclusions

We presented the numerical dispersion analysis of the Smoothed Particle Hydrodynamics applied to the one-dimensional isothermal gas dynamics equation. We confirmed theoretically that the SPH solution converges to the plane wave solution only when both numbers of neighbor particles tend to infinity and smoothing length tends to zero. We demonstrated visually that if the arbitrary number of the neighbor is fixed and the smoothing length tends to zero, the error tends to a value dependent on the number of neighbors, but not necessarily zero. In one-dimensional simulations, convergence with respect to spatial discretization is achieved in the classical sense for a countable number of values of $\Delta x/H$. According to the numerical analysis, if the method converges, it possesses the second order of convergence with respect to grid step (stencil length).

Moreover, we demonstrated the ability of dispersion analysis to explain some numerical artifacts of SPH with coarse resolution. In particular, we found regimes with pronounced dispersion of sound waves in the wave package and delay of the wave package as a whole. Finally, our theoretical predictions are confirmed in simulations.

References

1. Ainsworth, M.: Discrete dispersion relation for HP-version finite element approximation at high wave number. SIAM J. Numer. Anal. **42**(2), 553–575 (2004)
2. Ainsworth, M.: Dispersive and dissipative behaviour of high order discontinuous Galerkin finite element methods. J. Comput. Phys. **198**(1), 106–130 (2004)
3. Ainsworth, M., Wajid, H.A.: Dispersive and dissipative behavior of the spectral element method. SIAM J. Numer. Anal. **47**(5), 3910–3937 (2009)
4. Cha, S.-H., Whitworth, A.P.: Implementations and tests of Godunov-type particle hydrodynamics. Mon. Not. R. Astron. Soc. **340**, 73–90 (2003)
5. Cohen, G. (ed.): Metodes numeriques d'ordre eleve pour les ondes en regime transitoire. INRIA (1994). (in French)
6. Dehnen, W., Aly, H.: Improving convergence in smoothed particle hydrodynamics simulations without pairing instability. Mon. Not. R. Astron. Soc. **425**, 1068–1082 (2012)
7. Gingold, R.A., Monaghan, J.J.: Smoothed particle hydrodynamics: theory and application to non-spherical stars. Mon. Not. R. Astron. Soc. **181**, 375–89 (1977)
8. Grigoryev, V., Stoyanovskaya, O., Snytnikov, N.: Supercomputer model of dynamical dusty gas with intense momentum transfer between phases based on OpenFPM library. J. Phys: Conf. Ser. **2099**, 012056 (2021). https://doi.org/10.1088/1742-6596/2099/1/012056
9. Hubber, D.A., Rosotti, G.P., Booth, R.A.: GANDALF - Graphical Astrophysics code for N-body dynamics and Lagrangian fluids. Mon. Not. R. Astron. Soc. **473**, 1603–1632 (2018)
10. Lisitsa, V.: Dispersion analysis of discontinuous Galerkin method on triangular mesh for elastic wave equation. Appl. Math. Model. **40**, 5077–5095 (2016). https://doi.org/10.1016/j.apm.2015.12.039
11. Liu, Y.: Optimal staggered-grid finite-difference schemes based on least-squares for wave equation modelling. Geophys. J. Int. **197**(2), 1033–1047 (2014)

12. Lucy, L.B.: A numerical approach to the testing of the fission hypothesis. Astron. J. **82**, 1013–24 (1977)
13. Mazzieri, I., Rapetti, F.: Dispersion analysis of triangle-based spectral element methods for elastic wave propagation. Numer. Algorithms **60**(4), 631–650 (2012)
14. Monaghan, J.J.: On the problem of penetration in particle methods. J. Comput. Phys. **82**(1), 1–15 (1989)
15. Monaghan, J.J.: Smoothed particle hydrodynamics. Rep. Prog. Phys. **68**, 1703–1759 (2005). https://doi.org/10.1088/0034-4885/68/8/R01
16. Morris, J.P.: A study of the stability properties of smooth particle hydrodynamics. Publ. Astron. Soc. Austral. **13**(1), 97–102 (1996)
17. Mulder, W.A.: Spurious modes in finite-element discretizations of the wave equation may not be all that bad. Appl. Numer. Math. **30**(4), 425–445 (1999)
18. Price, D.J.: Smoothed particle hydrodynamics and magnetohydrodynamics. J. Comput. Phys. **231**(3), 759–794 (2012)
19. Price, D., et al.: Phantom: a smoothed particle hydrodynamics and magnetohydrodynamics code for astrophysics. Publ. Astron. Soc. Austral. **35**, e031 (2020)
20. Rasio, F.A.: Particle methods in astrophysical fluid dynamics. Prog. Theor. Phys. Suppl. **138**, 609–621 (2000)
21. Quinlan, N.J., Basa, M., Lastiwka, M.: Truncation error in mesh-free particle methods. International journal for numerical methods in engineering Int. J. Numer. Meth. Eng. **66**, 2064–2085 (2006)
22. Springel, V.: The cosmological simulation code gadget-2. Mon. Not. R. Astron. Soc. **364**(4), 1105–1134 (2005)
23. Stoyanovskaya, O.P., Glushko, T.A., Snytnikov, N.V., Snytnikov, V.N.: Two-fluid dusty gas in smoothed particle hydrodynamics: fast and implicit algorithm for stiff linear drag. Astron. Comp. **25**, 25–37 (2018)
24. Stoyanovskaya, O.P., Davydov, M., Arendarenko, M., Isaenko, E., Markelova, T., Snytnikov, V.: Fast method to simulate dynamics of two-phase medium with intense interaction between phases by smoothed particle hydrodynamics: gas-dust mixture with polydisperse particles, linear drag, one-dimensional tests. J. Comp. Phys. **430**, 110035 (2021)
25. Vacondio, R., et al.: Grand challenges for smoothed particle hydrodynamics numerical schemes. Comput. Particle Mech. **8**(3), 575–588 (2020). https://doi.org/10.1007/s40571-020-00354-1
26. Zhang, C., et al.: SPHinXsys: an open-source meshless, multi-resolution and multiphysics library. Softw. Impacts **6**, 100033 (2020)
27. Zhu, Q., Hernquist, L., Li., Y.: Numerical convergence in smoothed particle hydrodynamics. Astrophys. J. **800**, Number 1 (2015)
28. LS-DYNA Homepage. https://www.lstc.com/products/ls-dyna. Accessed 2 Mar 2022